

# Universal Joint Source-Channel Coding for Modulation-Agnostic Semantic Communication

Yoon Huh, *Graduate Student Member, IEEE*, Hyowoon Seo, *Member, IEEE*, and Wan Choi, *Fellow, IEEE*

**Abstract**—From the perspective of joint source-channel coding (JSCC), there has been significant research on utilizing semantic communication, which inherently possesses analog characteristics, within digital device environments. However, a single-model approach that operates modulation-agnostically across various digital modulation orders has not yet been established. This article presents the first attempt at such an approach by proposing a universal joint source-channel coding (uJSCC) system that utilizes a single-model encoder-decoder pair and trained vector quantization (VQ) codebooks. To support various modulation orders within a single model, the operation of every neural network (NN)-based module in the uJSCC system requires the selection of modulation orders according to signal-to-noise ratio (SNR) boundaries. To address the challenge of unequal output statistics from shared parameters across NN layers, we integrate multiple batch normalization (BN) layers, selected based on modulation order, after each NN layer. This integration occurs with minimal impact on the overall model size. Through a comprehensive series of experiments, we validate that this modulation-agnostic semantic communication framework demonstrates superiority over existing digital semantic communication approaches in terms of model complexity, communication efficiency, and task effectiveness.

**Index Terms**—semantic communication, modulation-agnostic, joint source-channel coding, vector quantization.

## I. INTRODUCTION

We now have access to intelligent services encompassing smart X (e.g., home, city, vehicle factory, healthcare, etc.) and extended (augmented and virtual) reality, previously confined to the realm of imagination. However, the widespread adoption of such services faces a significant obstacle from the perspective of communication engineering. This challenge pertains to meeting user demands, often referred to as quality of experience (QoE), by efficiently and swiftly transmitting vast amounts of data. In response, sixth-generation (6G) communication has emerged to address these demands, heralding an anticipated paradigm shift from data-oriented to service (or task)-oriented communication [1].

A pivotal driver of this transition is semantic communication [2]–[4], evolving in tandem with advancements in machine learning (ML). Semantic communication targets the resolution of Level B (semantic) and Level C (effectiveness) communication issues [5], [6], with task-oriented joint source-channel coding (JSCC) at its core [7]–[10]. Unlike traditional communication systems, which segregate source coding and channel

coding modules, often with some loss of optimality, semantic communication, geared towards enhancing task performance, underscores an undeniable optimality gap in such modular separation. Consequently, current research in semantic communication focuses on harnessing ML capabilities to jointly optimize task execution, source coding, and channel coding, culminating in the implementation of neural network (NN)-based JSCC encoder-decoder pairs.

The challenge lies in the nature of NN training reliant on backpropagation, necessitating the exploration of JSCC techniques to facilitate the exchange of feature vectors within a continuous vector space between encoders and decoders. Although the implementation of semantic communication through analog transceivers might appear straightforward, it faces significant compatibility issues with the prevailing digital device infrastructure. An alternative strategy involves encoding the entries of feature vectors at the bit level and utilizing traditional digital modulation techniques. However, this approach is often inefficient, diminishing the benefits associated with semantic communication. Therefore, for effective semantic communication within a digital context, it is essential to incorporate digital modulation into the JSCC design considerations.

In the contemporary research landscape, innovative methods have been developed, notably the application of vector quantization (VQ) to the output feature vectors of encoders, followed by conventional digital modulation schemes (e.g., BPSK, 4QAM, 16QAM) or machine learning (ML)-based modulation utilizing a trained constellation map. These approaches, cited in recent studies [11]–[13], demonstrate robust performance within a specific modulation order. Yet, the goal of achieving consistent semantic communication performance across various modulation orders—a concept termed *modulation-agnostic semantic communication*<sup>1</sup>—requires a comprehensive suite of JSCC encoder-decoder pairs. In general, the optimal modulation order is contingent upon the channel environment, and maintaining this flexibility is often inefficient in terms of learning and hardware costs, including memory usage. Consequently, the pursuit of a universal framework capable of operating seamlessly across different modulation orders remains crucial for enhancing efficiency.

In response to the outlined challenges, this article introduces a novel framework for modulation-agnostic semantic communication, which is anchored in a single-model universal JSCC scheme that is adept at functioning across various modulation orders. To realize this, an NN-based uJSCC encoder-decoder

<sup>1</sup>Throughout this article, the modulation techniques discussed all pertain to digital modulation, and modulation-agnostic semantic communication refers to a digital semantic communication system designed to transmit or receive information without being constrained by any specific modulation scheme.

Y. Huh and W. Choi are with the Department of Electrical and Computer Engineering and the Institute of New Media and Communications, Seoul National University (SNU), Seoul 08826, Korea (e-mail: {mnhuh621, wanchoi}@snu.ac.kr)

H. Seo is with the Department of Electronics and Communications, Kwangju University, Seoul, Korea (e-mail: hyowoonseo@kw.ac.kr)

(Corresponding Authors: Hyowoon Seo and Wan Choi)

pair in conjunction with a VQ codebook is developed to utilize conventional digital modulation schemes. Notably, our proposed single-model encoder-decoder system demonstrates effective communication and task performance while maintaining reduced model complexity and training overhead compared to other benchmark approaches. In addition, the VQ codebook is not uniformly designed but is trained jointly with the uJSCC encoder-decoder, ensuring robust transmission of the extracted feature vectors.

The proposed framework is validated through a series of experiments in a semantic communication setting for image transmission and reconstruction tasks. We compare the proposed uJSCC against benchmark schemes, including model-efficient JSCC (which leverages a single model trained simultaneously for all modulation orders) and task-effective JSCC (which independently trains multiple models for each modulation order). The proposed scheme outperforms the model-efficient approach and achieves comparable or superior task performance compared to the task-effective JSCC by employing multiple batch normalization (BN) modules at each CNN layer. Furthermore, experiments demonstrate that the proposed method consistently delivers excellent performance across different encoder-decoder model sizes and with a higher volume of symbol transmission.

#### A. Related works

1) *Digital Semantic Communication*: A recent study [11] introduced a deterministic encoder-decoder pair in a digital semantic communication system using a VQ-variational autoencoder (VQ-VAE) [14] trained with a straight-through estimator and a vision transformer [15] backbone. The system enhances robustness against semantic noise through adversarial training and selective masking of non-critical image patches, identified via a feature importance module. However, there is a mismatch between codebook cardinality and modulation order, requiring two 16QAM symbols to transmit one index from a 256-cardinality codebook.

In [12], the authors proposed a VQ-based JSCC system employing digital modulation and an information bottleneck (IB) [16] loss function. This loss function's hyperparameter regulates the balance between task-relevant information and coded redundancy, thereby adjusting codebook robustness. During training, they utilized Gumbel-softmax [17], using the inner product between feature vectors and codewords as logits. This results in stochastic encoding, where codeword indices are sampled based on logits. However, despite the IB-optimized number of encoded bits, the actual transmission did not reflect this because both codebook cardinality and modulation order were fixed. Similarly, the encoder in [13] generates complex values, with symbols sampled based on logits from distances between complex output values and constellation map symbols. Another approach in [18] involved a stochastic encoder trained with a mutual information-based loss function, also utilizing Gumbel-softmax during training. In this system, symbols are directly sampled from output logits, eliminating the need for a learned codebook. However, these studies [12], [13], [18] face limitations in adapting to

multiple modulation orders as they require different neural network-based encoder-decoder parameter pairs for each order.

2) *Modulation-Agnostic Semantic Communication*: In recent work [19], the optimization of modulation order was addressed by solving a robustness verification problem to achieve a certain robustness probability, following the training of a semantic encoder and decoder. Another study [20] optimized the channel coding rate for conventional LDPC channel code through a similar robustness verification problem. This work utilized the CROWN method [21] to assess feature importance and measure output perturbation gaps from pretrained semantic encoders and decoders. As a separate source-channel coding system was employed, modulation order was aligned with the coding rate. However, both [19] and [20] did not incorporate digital modulation in the training of their encoders and decoders; instead, they applied fixed-bit quantization to analog outputs from the semantic encoder during inference to facilitate digital modulation, indicating a lack of joint design with the digital communication framework.

Meanwhile, [22] describes a system where a stochastic encoder produces logits to sample bits, thereby creating bit sequences. The authors used a binary symmetric erasure channel in their training scenario, simplifying the process by assuming a 4QAM context. Following training, the modulation order is adjusted according to channel SNR, with thresholds established based on predetermined robustness levels for each bit position. These levels are taken into account during training as well. However, the rationale behind training under 4QAM conditions was not clearly articulated, and the determination of robustness levels and SNR threshold adjustments was heuristic in nature, with the goal of achieving a smooth performance curve at the cost of increased complexity in system design.

#### B. Contributions and Organization

The contributions of this article are summarized as follows:

- This study explores methodologies that enable semantic communication within digital communication environments. Notably, it proposes a modulation-agnostic semantic communication framework that incorporates all the digital modulation orders in training.
- The cornerstone of the proposed framework is a uJSCC scheme that operates based on a trained encoder-decoder pair and a VQ codebook. This uJSCC scheme is capable of maintaining semantic communication as the optimal modulation order adjusts to varying channel conditions. To the best of our knowledge, this article presents the first instance of using a uJSCC scheme as a universal model capable of digitalizing semantic communication across multiple modulation orders.
- Through extensive experimentation, we demonstrate that the proposed uJSCC surpasses other benchmark schemes—including model-efficient and task-effective approaches—in terms of model and training complexity, as well as task performance.
- The numerical results illustrate that the proposed model achieves satisfactory reconstruction quality across all signal-to-noise ratio (SNR) ranges, utilizing an efficiently

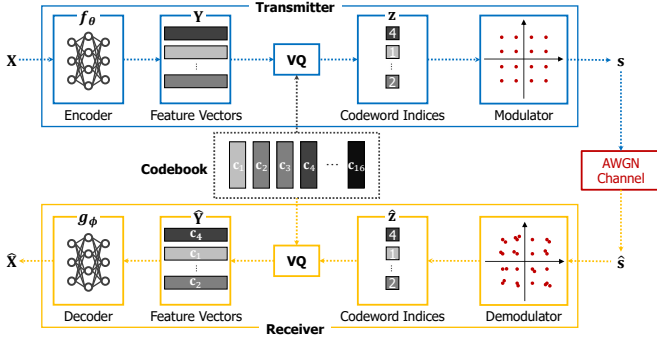


Fig. 1. An illustration of a JSCC and VQ-based digital semantic communication system model with 16QAM.

trained universal NN structure. Further analysis confirms that uJSCC can be effectively optimized for larger model sizes and in scenarios involving the transmission of more symbols, thereby highlighting the generality of the proposed system with fewer parameters.

The remainder of the article is structured as follows. Section II introduces the system model and the problem under investigation, along with a discussion of benchmark schemes. In Section III, we present a modulation-agnostic semantic communication framework that employs a uJSCC approach, detailing its implementation, modulation order selection, and training algorithm. Section IV discusses the extensive experimental results that validate the performance of the proposed scheme. Finally, conclusions are drawn in Section V.

### C. Notations

Vectors and matrices are expressed in bold lower-case and bold upper-case, respectively.  $\|\cdot\|_2$  denotes the  $l_2$  norm of a vector.  $\mathbb{R}$  and  $\mathbb{Z}$  represent, respectively, the real number set and integer set.  $[a:b]$  is a integer set of  $\{a, a+1, \dots, b\}$ .  $[\cdot]^T$  denotes the transpose of a matrix or vector.  $[\mathbf{A}]_{i:j,k:l}$  and  $[\mathbf{a}]_{i:j}$  represents, respectively, the sliced matrix of  $\mathbf{A}$  with row indices from  $i$  to  $j$  and column indices from  $k$  to  $l$ , and the sliced vector of  $\mathbf{a}$  with indices from  $i$  to  $j$ .  $\mathcal{CN}(\boldsymbol{\mu}, \boldsymbol{\Sigma})$  is complex normal distribution with mean vector  $\boldsymbol{\mu}$  and covariance matrix  $\boldsymbol{\Sigma}$ .  $\mathbf{I}_m$  is  $m \times m$  identity matrix.  $\mathbf{E}[\cdot]$  denotes the expected value of a given random variable.

## II. PRELIMINARIES

This section furnishes preliminary information concerning the system model, the problem under investigation, and benchmark schemes.

### A. System Description

Consider a point-to-point semantic communication system designed for image transmission tasks, incorporating JSCC encoder-decoder, vector quantizer-dequantizer, and modulator-demodulator pairs, as depicted in Fig. 1. For the sake of clarity and initial exposition, we presume a fixed digital modulation scheme characterized by order  $m$ . However, we subsequently investigate the system's adaptability to accommodate a spectrum of modulation order options. The operational structure

and functionality of this system are delineated comprehensively below.

The transmitter encodes a source image  $\mathbf{X} \in \mathbb{R}^{C \times H \times W}$ , where  $C$ ,  $H$ , and  $W$  are the number of channels, the height and width of the source image, respectively, into  $N$  feature vectors of  $D$  dimensions  $\mathbf{Y} = [\mathbf{y}_1, \mathbf{y}_2, \dots, \mathbf{y}_N]^T \in \mathbb{R}^{N \times D}$  via an encoder  $f_\theta$  parameterized by  $\theta$ , such that  $\mathbf{Y} = f_\theta(\mathbf{X})$ . Then, VQ is done utilizing a codebook with  $m$  codewords  $\mathbf{C} = [\mathbf{c}_1, \mathbf{c}_2, \dots, \mathbf{c}_m]^T \in \mathbb{R}^{m \times D}$  with the minimum distance criterion, i.e., the codeword index  $z_i$  for the  $i$ -th feature vector  $\mathbf{y}_i$  is chosen as  $z_i = \arg \min_j \|\mathbf{y}_i - \mathbf{c}_j\|_2^2$ .

Each codeword is mapped one-to-one to a symbol on a given modulation constellation map  $\mathbb{S} = \{\mathbf{s}_1, \mathbf{s}_2, \dots, \mathbf{s}_m\}$ , where  $\mathbf{s}_i \in \mathbb{R}^2$  and  $\mathbf{E}[\|\mathbf{s}_i\|_2^2] = P$  for all  $i \in [1:m]$ . The index vector  $\mathbf{z} = [z_1, z_2, \dots, z_N]^T \in [1:m]^N$  is modulated into a symbol sequence  $\mathbf{s} = [\mathbf{s}_{z_1}, \mathbf{s}_{z_2}, \dots, \mathbf{s}_{z_N}] \in \mathbb{S}^N$  and sent through an additive white Gaussian noise (AWGN) channel. At the receiver side, the receiver gets the symbol sequence with AWGN noise  $\mathbf{n} \sim \mathcal{CN}(0, \sigma^2 \mathbf{I}_N)$  as  $\hat{\mathbf{s}} = \mathbf{s} + \mathbf{n}$ , where SNR is calculated as  $\frac{P}{\sigma^2}$ . Then the receiver detects symbol sequence  $\bar{\mathbf{s}} = [\mathbf{s}_{\hat{z}_1}, \mathbf{s}_{\hat{z}_2}, \dots, \mathbf{s}_{\hat{z}_N}] \in \mathbb{S}^N$ , and dequantization is done from the detected index vector  $\hat{\mathbf{z}} = [\hat{z}_1, \hat{z}_2, \dots, \hat{z}_N]^T \in [1:m]^N$  utilizing the same codebook  $\mathbf{C}$  as the transmitter side, and then results in  $\hat{\mathbf{Y}} = [\mathbf{c}_{\hat{z}_1}, \mathbf{c}_{\hat{z}_2}, \dots, \mathbf{c}_{\hat{z}_N}]^T \in \mathbb{R}^{N \times D}$ . Finally, the receiver can reconstruct the image  $\hat{\mathbf{X}} \in \mathbb{R}^{C \times H \times W}$  from  $\hat{\mathbf{Y}}$  via a decoder  $g_\phi$ , parameterized by  $\phi$ , as

$$\hat{\mathbf{X}} = g_\phi(\hat{\mathbf{Y}}). \quad (1)$$

To optimize the system's operation, it is essential to train the encoder parameters  $\theta$ , decoder parameters  $\phi$ , and the codebook  $\mathbf{C}$ . This optimization is guided by the loss function proposed in [14], which encompasses three terms:

$$\mathcal{L} = \mathbf{E}_{\mathbf{X}}[e(\hat{\mathbf{X}}, \mathbf{X}) + \alpha e(\hat{\mathbf{Y}}, \mathbf{Y}_d) + \beta e(\mathbf{Y}, \hat{\mathbf{Y}}_d)], \quad (2)$$

where  $e(x, y)$  denotes the mean squared error between  $x$  and  $y$ , and  $\mathbf{A}_d$  represents duplicated versions of  $\mathbf{A}$ . This duplication is implemented to inhibit the flow of gradients through  $\mathbf{A}$ , thereby preventing updates to  $\mathbf{A}$  or the NN parameters involved in computing the matrix. The parameters  $\alpha$  and  $\beta$  serve as hyperparameters that regulate the relative significance of the respective loss components. The role of each component is summarized as follows.

- The first term pertains to the quality of the reconstruction task, albeit hindered by the inability to apply the chain rule in gradient calculation due to VQ. Consequently, leveraging the straight-through gradient estimator between  $\mathbf{Y}$  and  $\hat{\mathbf{Y}}$ , we establish a linkage between the gradient from  $e(\hat{\mathbf{X}}, \mathbf{X})$  to  $\hat{\mathbf{Y}}$  and the gradient from  $\mathbf{Y}$  to  $\mathbf{X}$ . This term significantly influences the training of both encoder parameter  $\theta$  and decoder parameter  $\phi$ .
- The second term aims to minimize the disparity between the detected codewords  $\hat{\mathbf{Y}}$  and the duplicated original feature vectors  $\mathbf{Y}_d$ , thereby guiding the training of the codebook  $\mathbf{C}$  alone.
- Due to challenges in achieving convergence of the codebook, the third term serves to regularize the training of the codebook  $\mathbf{C}$ , which is not directly related to the update

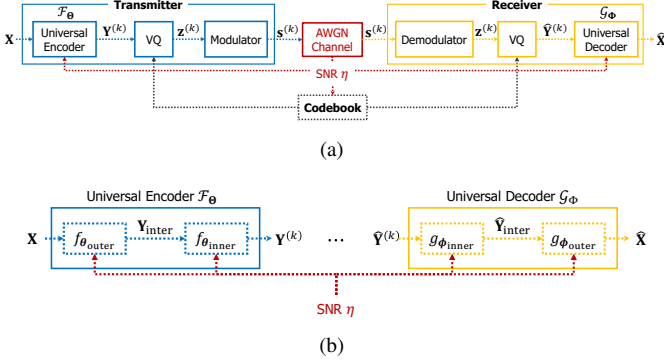


Fig. 2. The structures of (a) the proposed modulation-agnostic semantic communication system and (b) conceptually separated universal encoder and decoder.

of the codebook but the JSCC encoder. It achieves this by minimizing the disparity between the original feature vectors  $\mathbf{Y}$  and the duplicated detected codewords  $\hat{\mathbf{Y}}_d$ , thereby facilitating the alignment of the original feature vectors with the nearest codewords in the codebook.

Consequently, the parameters are obtained as

$$(\theta^*, \phi^*, \mathbf{C}^*) = \arg \min_{\theta, \phi, \mathbf{C}} \mathcal{L}. \quad (3)$$

During the training process, it is crucial to manage the hyperparameter  $\alpha$  with precision, while  $\beta$  usually works well setting to  $0.25\alpha$  [14]. If the sum of the second and third terms approaches zero too rapidly, the decoder will not receive sufficient training due to limited variation in the input codewords. In this scenario, reducing  $\alpha$  is advisable. Conversely, if the sum of the second and third terms remains excessively large, increasing  $\alpha$  is recommended since this indicates a substantial vector quantization error in the current codebook.

## B. Problem Formulation

In classical digital communication, a desired bit error rate (BER) or data rate is attained by adjusting the coding scheme or modulation order according to the channel conditions. Similarly, semantic communication could be envisioned to achieve optimal task performance by selecting the appropriate coding scheme or modulation order in response to the channel state.

Hence, the main target of this article is to develop a modulation-agnostic semantic communication framework, incorporating uJSCC encoder, decoder, and VQ codebook that support  $K$  different modulation orders, i.e.,  $m_1, m_2, \dots, m_K$ , where  $m_k$  represents the  $k$ -th modulation order and without loss of generality,  $m_1 < m_2 < \dots < m_K$ . In mathematical expression, let  $\mathbf{B} = [b_1, b_2, \dots, b_{K-1}]$  be the SNR boundary to choose modulation order among  $K$  types, where

$$m = \begin{cases} m_1, & \text{if } \eta < b_1, \\ m_k, & \text{if } b_{k-1} \leq \eta < b_k, \\ m_K, & \text{if } \eta \geq b_{K-1}, \end{cases} \quad (4)$$

where  $k \in [2:K-1]$ . The designing condition of the SNR boundary will be discussed in Section III-A.

Assume that both transmitter and receiver are aware of the SNR value  $\eta$ , enabling synchronization of the modulation order between the transmitter and receiver. The following communication process is conducted with respect to modulation order index  $k$  according to the SNR value  $\eta$ . As illustrated in Fig. 2(a), a universal encoder parameterized by  $\Theta$ , denoted by  $\mathcal{F}_\Theta$ , encodes a source image  $\mathbf{X}$  into feature vectors  $\mathbf{Y}^{(k)}$  given the SNR value  $b_{k-1} \leq \eta < b_k$ , such that  $\mathbf{Y}^{(k)} = \mathcal{F}_\Theta(\mathbf{X}, \eta) \in \mathbb{R}^{N \times D_k}$  where  $D_k$  is the dimension of feature vector of the modulation order  $m_k$ . The encoded feature vectors are quantized via codebook  $\mathbf{C}^{(k)}$  and modulated into symbols  $\mathbf{s}^{(k)}$ . The codebook for modulation order  $m_k$ , which should also be trained, can be expressed as

$$\mathbf{C}^{(k)} = [\mathbf{c}_1^{(k)}, \mathbf{c}_2^{(k)}, \dots, \mathbf{c}_{m_k}^{(k)}]^T \in \mathbb{R}^{m_k \times D_k}. \quad (5)$$

At the receiver, the received symbols  $\hat{\mathbf{s}}^{(k)}$  are detected and dequantized into  $\hat{\mathbf{Y}}^{(k)}$  via the same codebook  $\mathbf{C}^{(k)}$ . Finally, a universal decoder parameterized by  $\Phi$ , denoted as  $\mathcal{G}_\Phi$ , decodes  $\hat{\mathbf{Y}}^{(k)}$  into reconstructed image  $\hat{\mathbf{X}}$  given  $\eta$ , such that  $\hat{\mathbf{X}} = \mathcal{G}_\Phi(\hat{\mathbf{Y}}^{(k)}, \eta)$ .

The objective is to determine an optimal NN structure for the universal encoder  $\mathcal{F}_\Theta$  and universal decoder  $\mathcal{G}_\Phi$ , which include data processing paths for  $K$  modulation orders, codebook  $\mathbf{C}^{(k)}$  for all  $k \in [1:K]$ , and the SNR boundary  $\mathbf{B}$ . When designing this system, considerations include model complexity, the total number of NN parameters, training strategies, and task performance.

## C. Benchmark Schemes

Before delving into our proposed solution for the formulated problem above, we first introduce three benchmark schemes for comparison as follows.

1) *Model-Efficient JSCC*: The first and second benchmark schemes we introduce are what we refer to as the model-efficient (ME) JSCC. To minimize model complexity, this benchmark scheme utilizes a single encoder-decoder pair, but utilizes distinct VQ codebooks optimized for each modulation order. Given that higher modulation orders necessitate larger codeword dimensions, the codeword dimension  $D_k$  is standardized to  $D_K$  for all  $k \in [1:K]$  within this benchmark, such that  $\mathbf{Y}^{(k)} \in \mathbb{R}^{N \times D_K}$ , contrary to the proposed uJSCC. This approach enables a uniform representation across various modulation orders, simplifying model management and potentially reducing both training and operational complexities. The model can be trained using two distinct types of training strategies, details of which will be elaborated upon in the following.

The first strategy, dubbed  $ME_1$ , consists of single-stage training. It jointly trains to optimize the image reconstruction performance of all modulation orders and obtains a single encoder-decoder pair and  $K$  different codebooks for each modulation order. The loss function for the  $k$ -th modulation order can be represented as

$$\mathcal{L}_k = \mathbf{E}_{\mathbf{X}}[\mathbf{e}(\hat{\mathbf{X}}^{(k)}, \mathbf{X}) + \alpha_k \mathbf{e}(\hat{\mathbf{Y}}^{(k)}, \mathbf{Y}_d^{(k)}) + \beta_k \mathbf{e}(\mathbf{Y}^{(k)}, \hat{\mathbf{Y}}_d^{(k)})], \quad (6)$$

where the computation is done with the SNR value  $\eta$  randomly sampled from SNR range of the  $k$ -th modulation order. Then, the loss function to jointly train  $\text{ME}_1$  can be expressed as

$$\mathcal{L}^{\text{ME}_1} = \sum_{k=1}^K \lambda_k \mathcal{L}_k, \quad (7)$$

where  $\lambda_k$  is a hyperparameter to control the importance of loss terms for each modulation order.

The second strategy, termed  $\text{ME}_2$ , employs a double-stage training process. Initially,  $\text{ME}_2$  focuses on optimizing the performance of semantic communication for the  $K$ -th modulation order, which is the highest in the sequence. The loss function for this initial stage is given by:

$$\mathcal{L}_{(1)}^{\text{ME}_2} = \mathcal{L}_K. \quad (8)$$

Upon completion of the first stage, the second training stage commences. This stage is designed to optimize the codebooks  $\mathbf{C}^{(k)}$  for the remaining modulation orders, encompassing all  $k \in [1:K-1]$ , while keeping the encoder and decoder parameters fixed. The loss function for this second stage is defined as:

$$\mathcal{L}_{(2)}^{\text{ME}_2} = \sum_{k=1}^{K-1} \lambda_k \mathbf{E}_{\mathbf{X}}[\alpha_k e(\hat{\mathbf{Y}}^{(k)}, \mathbf{Y}_d^{(k)})]. \quad (9)$$

2) *Task-Effective JSCC*: The third benchmark aims to optimize the performance of JSCC for all SNR ranges. To this end, a set of encoder-decoder pair and codebook for each modulation order  $m_k$  should be trained independently with respect to  $k$ , different from ME approach and the proposed uJSCC. Then, during inference, a certain set for  $m_k$  is switched to be used among  $K$  sets, chosen according to the SNR value  $\eta$  and  $\mathbf{B}$ . Such an approach is dubbed *task-effective (TE)* approach. As the codebook cardinality for each modulation order increases with respect to  $k$ , we correspondingly scale the codeword dimensions  $D_k$  to increase in length, such that  $D_1 < D_2 < \dots < D_K$ . This escalation in codeword dimension is strategically designed to ensure that the image reconstruction performance is not compromised by VQ errors.

#### D. Discussions on Benchmark Schemes

The ME JSCC framework is capable of accommodating  $K$  different modulation orders using a single JSCC encoder-decoder pair, resulting in a parameter count that is approximately  $1/K$  times smaller than that of the TE JSCC. This significant reduction in parameters translates to a considerably simplified training process. In terms of training complexity, the ME JSCC strategies offer a more streamlined procedure compared to the TE JSCC. Specifically, for the  $\text{ME}_1$  approach, NN parameters for  $K$  different modulation orders are optimized simultaneously within a single epoch. In contrast, the TE approach involves sequential training for each modulation order, focusing individually on the corresponding encoder-decoder pairs. In the  $\text{ME}_2$  scenario, the initial training stage aligns with the TE approach, targeting the  $K$ -th modulation order. The subsequent stage, however, is less complex as it exclusively focuses on jointly training the codebooks for

TABLE I  
FEATURES OF UJSCC AND BENCHMARK SCHEMES

Scheme	# of Enc-Dec	$D_k$	Training	S-BN
uJSCC	1	Increasing order	Single	O
$\text{ME}_1$	1	$D_K$	Single	X
$\text{ME}_2$	1	$D_K$	Double	X
TE	$K$	Increasing order	Independent	X

the remaining modulation orders. This bifurcated approach not only simplifies the training process but also enhances efficiency by concentrating resources on refining the most impactful elements of the system.

From the perspective of task performance, TE JSCC is optimized to achieve superior performance across all SNR ranges. However, when considering the ME approaches, there are distinct limitations and performance boundaries. For the  $\text{ME}_1$  approach, its performance is inherently constrained by the use of parameter sharing across multiple modulation orders, leading to a ceiling effect dictated by the TE's capabilities. Furthermore, since the codeword dimension  $D_k$  is uniform across all modulation orders and set to  $D_K$ , the VQ error can be disproportionately large for lower modulation orders, adversely affecting performance. In the case of  $\text{ME}_2$ , while it may approximate the best performance for the  $K$ -th (highest) modulation order due to targeted optimization, the encoder-decoder pair is not optimized in conjunction with the codebooks for other modulation orders. Consequently, this decoupling limits its ability to ensure optimal performance across lower modulation orders, as the encoder-decoder configuration and the corresponding codebooks are not fine-tuned to work synergistically for each specific modulation context.

In summary, the presented solutions fail to simultaneously satisfy model efficiency and task effectiveness within the framework of modulation-agnostic semantic communication. Consequently, there is a clear necessity for a novel and efficient universal system design that not only achieves satisfactory task performance but also incorporates an appropriate training algorithm.

### III. MODULATION-AGNOSTIC UNIVERSAL JOINT SOURCE-CHANNEL CODING

This section presents a novel modulation-agnostic uJSCC scheme for digital semantic communication. A primary challenge in uJSCC development is the shared use of CNN parameters across multiple data processing paths for each modulation order, which can lead to statistical discrepancies and degrade performance. We address this issue by implementing a switchable batch normalization layer. The training methodology for the proposed uJSCC system is also detailed.

#### A. Universal Joint Source-Channel Coding

Before proceeding, it is essential to discuss the methodology for setting the SNR boundaries mentioned previously. In accordance with the 3GPP technical specification [23], the modulation and coding scheme (MCS) table delineates channel coding rates and modulation orders to maintain the block error rate (BLER) below 0.1. Our proposed system

utilizes a ML strategy to train the channel coding scheme across various digital modulation methods and corresponding SNR ranges. Also note that, in the proposed system, one symbol corresponds to a single feature vector which contains much more information than information-theoretic bits in one symbol. Inspired by [23], regarding a feature vector as the block in the conventional communication system, we establish SNR boundaries  $\mathbf{B} \in \mathbb{Z}^{K-1}$  aiming for a symbol error rate<sup>2</sup> (SER) [24] around 0.1. This adjustment adapts conventional communication standards to the feature vectors in our system, facilitating joint training of the uJSCC encoder-decoder pair and enhancing robustness against data compression and channel distortion. For example, with modulation types such as BPSK, 4QAM, 16QAM, 64QAM, and 256QAM, where  $K = 5$ , the SNR boundaries would be set at  $b_1 = 5$  dB,  $b_2 = 12$  dB,  $b_3 = 20$  dB, and  $b_4 = 26$  dB, respectively.

The proposed modulation-agnostic semantic communication structure incorporates a uJSCC encoder  $\mathcal{F}_\Theta$ , decoder  $\mathcal{G}_\Phi$ , and a quantizer/dequantizer based on codebooks  $\mathbf{C}^{(k)}$  for all  $k \in [1:K]$  as delineated in (5). For simplicity, the encoder and decoder are conceptually divided into inner and outer components. Specifically, as illustrated in Fig. 2(b), the encoder  $\mathcal{F}_\Theta$  comprises an outer encoder  $f_{\theta_{\text{outer}}}$  and an inner encoder  $f_{\theta_{\text{inner}}}$ , while the decoder  $\mathcal{G}_\Phi$  consists of an inner decoder  $g_{\phi_{\text{inner}}}$  and an outer decoder  $g_{\phi_{\text{outer}}}$ . Note that the roles of the inner encoder and decoder are to efficiently process the data, adaptive to the different required shapes of output and input, respectively, according to a chosen modulation order, while the roles of the outer encoder and decoder are preprocessing and postprocessing of the data, respectively, concerned with the inner coding process. Both the outer encoder and decoder are structured with multiple CNN layers, and the inner components are each composed of a single CNN layer. The detailed NN architectures for both the encoder and decoder will be described in Section IV and features of uJSCC and benchmark schemes are summarized in TABLE I. Additionally, the operation of the proposed JSCC system is explained in detail below and summarized in **Algorithm 1**.

The operational mechanism of the proposed uJSCC system is described in detail as follows. It is presupposed that the channel condition in SNR, denoted as  $\eta$ , is known in advance to both the transmitter and receiver, facilitating the predetermined selection of the modulation order  $m_k$  as delineated by (4) and consequently the index  $k$ . Initially, at the transmitter, the source image  $\mathbf{X}$  is encoded into intermediate feature vectors  $\mathbf{Y}_{\text{inter}} \in \mathbb{R}^{c_1 \times h_1 \times w_1}$  through the outer encoder, represented by  $f_{\theta_{\text{outer}}}$ :

$$\mathbf{Y}_{\text{inter}} = f_{\theta_{\text{outer}}}(\mathbf{X}, k). \quad (10)$$

The intermediate vectors are subsequently processed by the inner encoder  $f_{\theta_{\text{inner}}}$  tailored for the  $k$ -th modulation order. The inner encoder transforms these vectors into reshaped

<sup>2</sup>SNR boundaries can also be learnable. However, in this paper, we focus on implementing a universal system that approaches the TE's performance with a single encoder-decoder pair when all the schemes in this article use the same SNR boundaries.

---

**Algorithm 1** Universal Joint Source-Channel Coding

---

- 1: **Input:**  $\mathbf{X}$ ,  $\eta$ ,  $\mathbf{B} = [b_1, b_2, \dots, b_{K-1}]$ ,  $\mathcal{F}_\Theta$ ,  $\mathcal{G}_\Phi$ ,  $\mathbf{C}^{(k)}$  for  $k \in [1:K]$
  - 2: Choose  $m_k$  according to  $\eta$  and  $\mathbf{B}$  with (4)
  - 3: Encode source image  $\mathbf{X}$  into feature vectors  $\mathbf{Y}^{(k)}$  via  $\mathcal{F}_\Theta$  according to (12)
  - 4: Quantize  $\mathbf{Y}^{(k)}$  into codeword indices  $\mathbf{z}^{(k)}$  using  $\mathbf{C}^{(k)}$  according to (13)
  - 5: Modulate  $\mathbf{z}^{(k)}$  into symbol sequence  $\mathbf{s}^{(k)}$
  - 6: Transmit  $\mathbf{s}^{(k)}$  via AWGN channel with  $\eta$  as (14)
  - 7: Detect received values into  $\bar{\mathbf{s}}^{(k)}$  and get  $\hat{\mathbf{z}}^{(k)}$
  - 8: Dequantize  $\hat{\mathbf{z}}^{(k)}$  into  $\hat{\mathbf{Y}}^{(k)}$  using  $\mathbf{C}^{(k)}$
  - 9: Reconstruct  $\hat{\mathbf{X}}^{(k)}$  from  $\hat{\mathbf{Y}}^{(k)}$  via  $\mathcal{G}_\Phi$  according to (17)
  - 10: **Output:**  $\hat{\mathbf{X}}^{(k)}$
- 

feature vectors  $\mathbf{Y}^{(k)} = [\mathbf{y}_1^{(k)}, \mathbf{y}_2^{(k)}, \dots, \mathbf{y}_N^{(k)}]^T$ , appropriate for  $k \in [1:K]$ :

$$\mathbf{Y}^{(k)} = f_{\theta_{\text{inner}}}(\mathbf{Y}_{\text{inter}}, k), \quad (11)$$

where  $\theta_{\text{inner}}$  denotes the NN parameters of the inner encoder. This encoder features a single CNN layer and operates with computational efficiency to yield  $\mathbf{Y}^{(k)}$  in the desired configuration of  $N \times D_k$ . This process avoids simply slicing an output tensor of dimension  $N \times D_K$  and instead utilizes the capabilities of the inner encoder to adapt the dimensions effectively for each specific modulation order, contrary to the ME approach.

Let  $\theta_{\text{inner}}^{\text{CNN}} \in \mathbb{R}^{D_K \times c_1 \times f \times f}$  represent the tensor of CNN parameters in  $\theta_{\text{inner}}$ , where  $f \times f$  denotes the kernel size. This tensor comprises  $D_K$  convolutional filters, each of shape  $c_1 \times f \times f$ , which are applied to a zero-padded input tensor using striding techniques. Depending on the chosen modulation order  $m_k$ , only the first  $D_k$  filters, denoted as  $[\theta_{\text{inner}}^{\text{CNN}}]_{1:D_k, \dots, \dots}$ , are utilized by the CNN layer of the inner encoder for encoding purposes. As  $k$  increases, so does the dimension of the feature vector for each modulation order, with  $D_1 < D_2 < \dots < D_K$ , resulting in reduced computational load for lower modulation orders due to the utilization of fewer parameters. Consequently, the inner encoder requires  $2ND_k c_1 f^2$  floating-point operations (FLOPs) for encoding, in contrast to  $2ND_K c_1 f^2$  FLOPs when all filters are used, which is  $D_K/D_k$  times more. This sophisticated encoding process achieves the same data processing efficacy as an encoder specifically designed for the  $k$ -th modulation order, consistent with the TE approach. The universal encoder  $\mathcal{F}_\Theta$  can be mathematically expressed as follows:

$$\mathcal{F}_\Theta(\mathbf{X}, \eta) = f_{\theta_{\text{inner}}}(f_{\theta_{\text{outer}}}(\mathbf{X}, k), k). \quad (12)$$

Subsequently, VQ is performed using a codebook  $\mathbf{C}^{(k)}$ , which should also be optimized jointly with the encoder and decoder during training, based on the minimum distance criterion. For each  $i$ -th feature vector  $\mathbf{y}_i^{(k)}$ , a symbol index  $z_i^{(k)}$  is selected according to the following equation:

$$z_i^{(k)} = \arg \min_j \|\mathbf{y}_i^{(k)} - \mathbf{c}_j^{(k)}\|_2^2. \quad (13)$$

Each codeword  $\mathbf{c}_j^{(k)}$  corresponds one-to-one to a symbol  $\mathbf{s}_j^{(k)}$  indexed on the corresponding constellation map  $\mathbb{S}^{(k)}$ . An index vector  $\mathbf{z}^{(k)} = [z_1^{(k)}, z_2^{(k)}, \dots, z_N^{(k)}]^T$  is then modulated into a symbol sequence  $\mathbf{s}^{(k)} \in (\mathbb{S}^{(k)})^N$ , which is subsequently transmitted through an additive white Gaussian noise (AWGN) channel.

Upon receiving the symbol sequence altered by AWGN noise

$$\hat{\mathbf{s}}^{(k)} = \mathbf{s}^{(k)} + \mathbf{n}, \quad (14)$$

the receiver detects it into  $\bar{\mathbf{s}}^{(k)} \in (\mathbb{S}^{(k)})^N$ . Subsequently, vector dequantization is performed using the detected index vector  $\hat{\mathbf{z}}^{(k)} = [\hat{z}_1^{(k)}, \hat{z}_2^{(k)}, \dots, \hat{z}_N^{(k)}]^T$  and the same codebook  $\mathbf{C}^{(k)}$  employed at the transmitter, yielding the received feature vectors  $\hat{\mathbf{Y}}^{(k)}$ . These vectors are then decoded by the inner decoder  $g_{\phi_{\text{inner}}}$  into recovered intermediate feature vectors  $\hat{\mathbf{Y}}_{\text{inter}} \in \mathbb{R}^{c_1 \times h_1 \times w_1}$ , formulated as:

$$\hat{\mathbf{Y}}_{\text{inter}} = g_{\phi_{\text{inner}}}(\hat{\mathbf{Y}}^{(k)}, k), \quad (15)$$

where  $\phi_{\text{inner}}$  denotes the NN parameters of the inner decoder. This decoder, consisting of a single transpose CNN layer, efficiently processes  $\hat{\mathbf{Y}}^{(k)}$  without requiring zero-padding to conform to the shape  $N \times D_K$ , contrary to the ME approach.

Let  $\phi_{\text{inner}}^{\text{CNN}} \in \mathbb{R}^{D_K \times c_1 \times f \times f}$  denote the tensor of CNN parameters in  $\phi_{\text{inner}}$ , where  $f \times f$  represents the kernel size. This tensor comprises  $D_K$  transpose convolution filters, each of shape  $c_1 \times f \times f$ , while the  $i$ -th filter is applied to the  $i$ -th channel of the input tensor via the Kronecker product, followed by striding, summation, and edge cutting for size adjustment. Similarly to the encoder, the inner decoder employs only the first  $D_k$  filters, denoted as  $[\phi_{\text{inner}}^{\text{CNN}}]_{1:D_k, \dots, \dots}$ , for decoding, corresponding to the modulation order  $m_k$ . This selective filter usage necessitates  $2ND_k c_1 f^2$  FLOPs for lower modulation orders, in contrast to  $2ND_K c_1 f^2$  FLOPs required if all filters were utilized. This optimized decoding process mirrors the efficiency of a decoder specifically tailored for the  $k$ -th modulation order, consistent with the TE approach.

Finally, the receiver reconstructs the image  $\hat{\mathbf{X}}^{(k)}$  from  $\hat{\mathbf{Y}}_{\text{inter}}$  using the outer decoder  $g_{\phi_{\text{outer}}}$ , described as:

$$\hat{\mathbf{X}}^{(k)} = g_{\phi_{\text{outer}}}(\hat{\mathbf{Y}}_{\text{inter}}, k), \quad (16)$$

where  $\phi_{\text{outer}}$  are the NN parameters of the outer decoder. The overall operation of the universal decoder  $\mathcal{G}_{\Phi}$  is encapsulated by:

$$\mathcal{G}_{\Phi}(\hat{\mathbf{Y}}, \eta) = g_{\phi_{\text{outer}}}(g_{\phi_{\text{inner}}}(\hat{\mathbf{Y}}^{(k)}, k), k). \quad (17)$$

### B. Switchable Batch Normalization Layer

Batch normalization (BN) layers [25] significantly facilitate the training of NN models and enhance their performance by standardizing the statistics of an output tensor from each NN layer. This ensures that subsequent layers receive inputs with consistent statistical properties during each forward pass.

Let  $\mathbf{T}^{(n,i)}$  denote the  $i$ -th channel of the output tensor from the  $n$ -th NN layer, and let  $t_j^{(n,i)}$  represent its  $j$ -th element, both pertaining to a single mini-batch. The BN layer first normalizes each  $t_j^{(n,i)}$  into a normalized value  $\hat{t}_j^{(n,i)}$  using

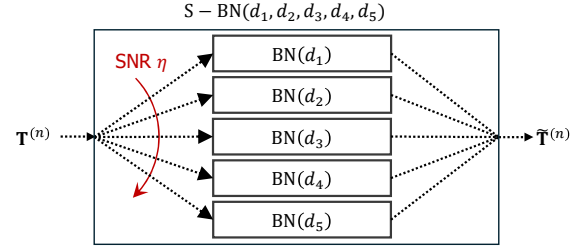


Fig. 3. An illustration of switchable batch normalization layer with five paths.

the mini-batch mean  $\mu^{(n,i)}$  and standard deviation  $\sigma^{(n,i)}$ . The normalized values are then scaled and biased to produce the batch-normalized value  $\hat{t}_j^{(n,i)}$ , as described by the following equations:

$$\mu^{(n,i)} = \mathbf{E}_j [t_j^{(n,i)}], \quad (18)$$

$$\sigma^{(n,i)} = \sqrt{\mathbf{E}_j \left[ \left( t_j^{(n,i)} - \mu^{(n,i)} \right)^2 \right]}, \quad (19)$$

$$\hat{t}_j^{(n,i)} = \frac{t_j^{(n,i)} - \mu^{(n,i)}}{\sigma^{(n,i)} + \epsilon}, \quad (20)$$

$$\tilde{t}_j^{(n,i)} = \gamma^{(n,i)} \hat{t}_j^{(n,i)} + \beta^{(n,i)}, \quad (21)$$

where  $\gamma^{(n,i)}$  and  $\beta^{(n,i)}$  are the parameters learned for rescaling and bias adjustment, respectively, and  $\epsilon$  is a small constant for numerical stability.

During inference, where batch-level computations are absent, the mean  $\mu^{(n,i)}$  and standard deviation  $\sigma^{(n,i)}$  from the training phase are replaced with running estimates  $\bar{\mu}^{(n,i)}$  and  $\bar{\sigma}^{(n,i)}$ , calculated via a moving average:

$$\hat{t}_j^{(n,i)} = \frac{t_j^{(n,i)} - \bar{\mu}^{(n,i)}}{\bar{\sigma}^{(n,i)} + \epsilon}, \quad (22)$$

$$\tilde{t}_j^{(n,i)} = \gamma^{(n,i)} \hat{t}_j^{(n,i)} + \beta^{(n,i)}, \quad (23)$$

Simplified expressions during inference are:

$$\tilde{\gamma}^{(n,i)} = \frac{\gamma^{(n,i)}}{\bar{\sigma}^{(n,i)} + \epsilon}, \quad (24)$$

$$\tilde{\beta}^{(n,i)} = \beta^{(n,i)} - \tilde{\gamma}^{(n,i)} \bar{\mu}^{(n,i)}, \quad (25)$$

$$\tilde{t}_j^{(n,i)} = \tilde{\gamma}^{(n,i)} t_j^{(n,i)} + \tilde{\beta}^{(n,i)}, \quad (26)$$

which require only two adjusted variables per channel.

The architecture of the proposed model integrates a BN layer following each CNN layer. Given that the proposed uJSCC model's input tensor size for the inner decoder  $g_{\phi_{\text{inner}}}$  varies with each modulation order, it is essential to manage the differing statistics of the output tensor across modulation orders. To accommodate the  $K$  different modulation orders in uJSCC, we employ  $K$  specific BN layers, each configured to manage the statistics for its respective data processing path, thus maintaining optimal task performance despite modulation-agnostic characteristics, which is the biggest difference with the ME approach. Furthermore, this variability in statistics impacts other CNN layers, necessitating  $K$  switchable BN (S-BN) layers post each CNN layer, selected

---

**Algorithm 2** uJSCC Training Algorithm
 

---

```

1: Input:  $\mathcal{D}$ ,  $\mathbf{B}_{\text{train}} = [b_0, b_1, \dots, b_K]$ ,  $(\alpha_k, \beta_k, \lambda_k)$  for  $k \in [1:K]$ ,  $I_{\text{max}}$ 
2: Initialize:  $\Theta = \{\theta_{\text{outer}}, \theta_{\text{inner}}\}$ ,  $\Phi = \{\phi_{\text{outer}}, \phi_{\text{inner}}\}$ ,  $\mathbf{C}^{(k)}$  for  $k \in [1:K]$ 
3:  $\varphi \leftarrow \{\Theta, \Phi, \mathbf{C}^{(1)}, \mathbf{C}^{(2)}, \dots, \mathbf{C}^{(K)}\}$ 
4:  $i = 0$  ▷ Iteration index
5: while  $i < I_{\text{max}}$  or early stopping criterion is not met do
6:    $\mathbf{J} = [ ]$  ▷ Empty array
7:   for  $k = 1:K$  do
8:     Sample  $\eta$  such that  $b_{k-1} \leq \eta < b_k$ 
9:     Append  $\eta$  into  $\mathbf{J}$ 
10:  end for
11:   $\mathcal{L}_{\text{total}} = 0$  ▷ Clear loss value
12:  for  $\eta$  in  $\mathbf{J}$  do
13:    Choose  $m_k$  according to  $\eta$  and  $\mathbf{B}_{\text{train}}$  with (4)
14:    Compute  $\mathcal{L}_k$  via Algorithm 1 and (6)
15:     $\mathcal{L}_{\text{total}} \leftarrow \mathcal{L}_{\text{total}} + \lambda_k \mathcal{L}_k$ 
16:  end for
17:  Update  $\varphi$  via Adam [27] optimizer using  $\mathcal{L}_{\text{total}}$  of (27)
18:   $i \leftarrow i + 1$ 
19: end while
20: Output:  $\varphi$ 

```

---

based on the modulation order  $m_k$ . This multi-layered S-BN concept, referred to in [26], ensures model efficiency given that the parameter count of S-BN is minimal compared to the total model parameters. For example, with  $K = 5$ , as illustrated in Fig. 3, S-BN( $d_1, d_2, d_3, d_4, d_5$ ) comprises five BN layers, each corresponding to a different dimension  $\{d_1, d_2, d_3, d_4, d_5\}$ .

### C. Training Strategy

The training procedure for the uJSCC system is conducted jointly across all modulation orders. This method optimizes the universal encoder parameters  $\Theta = \{\theta_{\text{outer}}, \theta_{\text{inner}}\}$ , universal decoder parameters  $\Phi = \{\phi_{\text{outer}}, \phi_{\text{inner}}\}$ , and codebooks  $\mathbf{C}^{(k)}$  for  $k \in [1:K]$ . The overall training process is outlined below and summarized in **Algorithm 2**.

The training utilizes a dataset  $\mathcal{D}$ , with hyperparameters such as  $\alpha_k, \beta_k$ , and  $\lambda_k$ , and an SNR boundary  $\mathbf{B}_{\text{train}}$ , which includes upper and lower bounds added to  $\mathbf{B}$  for training conditions. All parameters are initialized before training begins. For each training cycle, one SNR value per modulation order for all  $k \in [1:K]$  is sampled. The corresponding loss value  $\mathcal{L}_k$  is computed for each SNR using **Algorithm 1** according to the modulation loss function (6). The overall system is trained jointly, and the total loss is computed as:

$$\mathcal{L}_{\text{total}} = \sum_{k=1}^K \lambda_k \mathcal{L}_k, \quad (27)$$

where  $\lambda_k$  weighs the importance of the loss terms for each modulation order. Parameter updates are performed using the Adam optimizer [27] based on  $\mathcal{L}_{\text{total}}$ . The training process continues iteratively until the maximum number of iterations is

reached or an early stopping criterion is met, ensuring optimal parameter optimization across the system.

## IV. EXPERIMENTAL RESULTS

This section evaluates the uJSCC scheme's performance in an AWGN channel, assuming perfect channel knowledge at both the transmitter and receiver. Benchmark schemes ME<sub>1</sub>, ME<sub>2</sub>, and TE JSCC are assessed, as detailed in Section II-C. The task of image reconstruction is quantified using peak SNR (PSNR) and the structural similarity index measure (SSIM) [28], with modulation schemes of BPSK, 4QAM, 16QAM, 64QAM, and 256QAM across modulation orders  $K = 5$ , where  $m_1 = 2$ ,  $m_2 = 4$ ,  $m_3 = 16$ ,  $m_4 = 64$ , and  $m_5 = 256$ .

The NN structure for the proposed model, for sizes  $N = 256$  and  $N = 1024$ , is detailed in TABLE II. Below, the notation used within this table is clarified:

- Conv( $c_{in}, c_{out}, f, s, p$ ): Represents a 2D convolutional layer with input channel  $c_{in}$ , output channel  $c_{out}$ , kernel size  $f$ , stride  $s$ , and padding  $p$ .
- T-Conv( $c_{in}, c_{out}, f, s, p$ ): A 2D transpose convolutional layer, parameterized similarly to the Conv layer.
- Res( $c$ ) and T-Res( $c$ ): Indicate a residual layer [29] and transpose residual layer, respectively, each preserving the input data's dimensions.
- Reshape: Used for reordering dimensions and altering dimensions via merging or splitting.
- ReLU and Tanh: Activation functions using rectified linear unit and hyperbolic tangent functions, respectively.

Training employs **Algorithm 2** with SNR boundary  $\mathbf{B}_{\text{train}} = [0, 5, 12, 20, 26, 30]$ . CIFAR-10 dataset [30] usage includes 50,000 training, with a 20% validation subset, and 10,000 test images. Training parameters include an initial learning rate of 0.001, halved every 20 epochs, a batch size of 64, and a maximum of  $I_{\text{max}} = 400$  epochs. Hyperparameters  $\alpha$  and  $\lambda$  are noted in TABLE III, with  $\beta$  fixed at  $0.25\alpha$ .

Three simulation configurations are established as follows:

- **Basic** (or **B**): This setup configures the number of symbols to  $N = 256$ . It features codeword dimensions  $(D_1, D_2, D_3, D_4, D_5) = (2, 4, 8, 12, 16)$  and NN channel counts  $(c_1, c_2) = (32, 64)$ .
- **Large** (or **L**): Maintaining the same number of symbols,  $N = 256$ , this configuration increases the codeword dimensions to  $(D_1, D_2, D_3, D_4, D_5) = (4, 8, 16, 24, 32)$  and adjusts the channel counts to  $(c_1, c_2) = (64, 32)$ . This effectively doubles the codeword dimensions and reconfigures the channel numbers relative to the **Basic** configuration.
- **More Symbols** (or **MS**): This configuration also sets the symbol count at  $N = 1024$  and retains the codeword dimensions and channel numbers of the **Basic** setup:  $(D_1, D_2, D_3, D_4, D_5) = (2, 4, 8, 12, 16)$  and  $(c_1, c_2) = (32, 64)$ . However, it increases the total number of transmitted symbols by fourfold compared to the **Basic** configuration.

Each configuration aims to evaluate the performance of the system under varying structural complexities and transmission capacities.



TABLE II  
NN STRUCTURE (“/” IS USED TO SEPARATELY DESCRIBE CASES  $N = 256$  AND  $N = 1024$ )

Module	Layers	Output size
Outer encoder	Conv(3, $c_1$ , 5, 1, 2) + S-BN( $c_1, c_1, c_1, c_1, c_1$ ) + ReLU	$c_1 \times 32 \times 32$
	Conv( $c_1, c_2, 5, 1, 2$ ) + S-BN( $c_2, c_2, c_2, c_2, c_2$ ) + ReLU	$c_2 \times 32 \times 32$
	Res( $c_2$ ) + ReLU	$c_2 \times 32 \times 32$
	Conv( $c_2, c_1, 2, 2, 0$ ) / Conv( $c_2, c_1, 5, 1, 2$ ) + S-BN( $c_1, c_1, c_1, c_1, c_1$ ) + ReLU	$c_1 \times 16 \times 16$ / $c_1 \times 32 \times 32$
Inner encoder	Res( $c_1$ ) + ReLU	$c_1 \times 16 \times 16$ / $c_1 \times 32 \times 32$
Inner decoder	Conv( $c_1, D_5, 5, 1, 2$ ) + S-BN( $D_1, D_2, D_3, D_4, D_5$ ) + Tanh + Reshape	$256 \times D_k$ / $1024 \times D_k$
Outer decoder	Reshape + T-Conv( $D_5, c_1, 5, 1, 2$ ) + S-BN( $c_1, c_1, c_1, c_1, c_1$ ) + ReLU	$c_1 \times 16 \times 16$ / $c_1 \times 32 \times 32$
	T-Res( $c_1$ ) + ReLU	$c_1 \times 16 \times 16$ / $c_1 \times 32 \times 32$
	T-Conv( $c_1, c_2, 2, 2, 0$ ) / T-Conv( $c_1, c_2, 5, 1, 2$ ) + S-BN( $c_2, c_2, c_2, c_2, c_2$ ) + ReLU	$c_2 \times 32 \times 32$
	T-Res( $c_2$ ) + ReLU	$c_2 \times 32 \times 32$
	T-Conv( $c_2, c_1, 5, 1, 2$ ) + S-BN( $c_1, c_1, c_1, c_1, c_1$ ) + ReLU	$c_1 \times 32 \times 32$
Res(c)	T-Conv( $c_1, 3, 5, 1, 2$ ) + S-BN(3, 3, 3, 3, 3) + Tanh	$3 \times 32 \times 32$
	Conv( $c, c, 3, 1, 1$ ) + S-BN( $c, c, c, c, c$ ) + ReLU	$c \times h \times w$
T-Res(c)	Conv( $c, c, 1, 1, 0$ ) + S-BN( $c, c, c, c, c$ )	$c \times h \times w$
	T-Conv( $c, c, 1, 1, 0$ ) + S-BN( $c, c, c, c, c$ ) + ReLU	$c \times h \times w$
	T-Conv( $c, c, 3, 1, 1$ ) + S-BN( $c, c, c, c, c$ )	$c \times h \times w$

TABLE III

HYPERPARAMETERS FOR TRAINING ( $\alpha$  AND  $\lambda$  FOR EACH MODULATION ARE WRITTEN SEQUENTIALLY IN INCREASING MODULATION ORDER. FOR ME<sub>2</sub>, THE FIRST STAGE IS FOR 256QAM AND THE SECOND STAGE IS FOR THE REST OF THE MODULATION ORDERS. NOTE THAT MULTIPLE  $\lambda$ -S ARE FOR JOINT TRAINING METHOD.)

Model		Hyper-parameters		
Setting	Scheme	$\alpha$	$\lambda$	
B	uJSCC	3, 1.5, 1, 0.7, 0.5	1, 1, 1, 1, 1	
	ME <sub>1</sub>	5, 4, 3, 2, 1.5	1, 1, 1, 4, 16	
	ME <sub>2</sub>	1	1	-
		2	5, 3, 2, 1	1, 1, 1, 1
	TE	4, 1, 1, 1, 1	-	
	uJSCC (( $c_1, c_2$ ) = (48, 96))	3, 1.5, 1, 0.7, 0.5	1, 1, 1, 4, 16	
uJSCC (( $c_1, c_2$ ) = (64, 128))	3, 2, 1, 0.7, 0.5	1, 1, 1, 4, 16		
L	uJSCC	3, 2, 1, 0.7, 0.5	1, 1, 2, 4, 16	
	ME <sub>1</sub>	5, 4, 3, 2, 1.5	1, 1, 1, 4, 16	
	ME <sub>2</sub>	1	1	-
		2	5, 3, 2, 1	1, 1, 1, 1
	SSN	4, 2, 1, 1, 1	-	
MS	uJSCC	3, 2, 1, 0.7, 0.5	1, 1, 1, 4, 16	
	ME <sub>1</sub>	5, 4, 3, 2, 1.5	1, 1, 1, 4, 16	
	ME <sub>2</sub>	1	1	-
		2	5, 3, 2, 1	1, 1, 1, 1
	TE	1, 1, 1, 1, 1	-	

TABLE IV

NUMBER OF PARAMETERS IN NN MODELS (THE RATIO OF BN PARAMETERS IS WRITTEN IN PERCENTAGE. THE RATIO OF THE TOTAL PARAMETERS COMPARED TO UJSCC IS WRITTEN IN MULTIPLE SCALES.)

Model		Number of parameters	
Setting	Scheme	BN (%)	Total
B	uJSCC	6514 (2.52%)	258098
	ME	1318 (0.54%)	252902 ( $\times 0.98$ )
	TE	6514 (0.52%)	1203634 ( $\times 4.66$ )
uJSCC (( $c_1, c_2$ ) = (48, 96))	9714 (1.76%)	552978 ( $\times 2.14$ )	
uJSCC (( $c_1, c_2$ ) = (64, 128))	12914 (1.35%)	958450 ( $\times 3.71$ )	
L	uJSCC	12998 (1.29%)	1009734
	ME	2630 (0.26%)	999366 ( $\times 0.99$ )
	TE	12998 (0.27%)	4753478 ( $\times 4.71$ )
MS	uJSCC	6514 (1.89%)	344114
	ME	1318 (0.39%)	338918 ( $\times 0.98$ )
	TE	6514 (0.40%)	1633714 ( $\times 4.75$ )

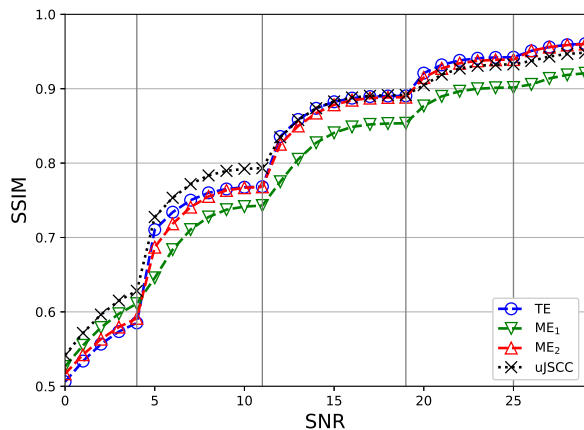
TABLE V

FLOPS AND TRAINING EPOCHS OF NN MODELS (FLOPS ARE WRITTEN IN “ENCODER FLOPS/DECODER FLOPS” FORMAT AND THE NUMBER OF EPOCHS OF TE IS SUMMED RIGHT SIDE.)

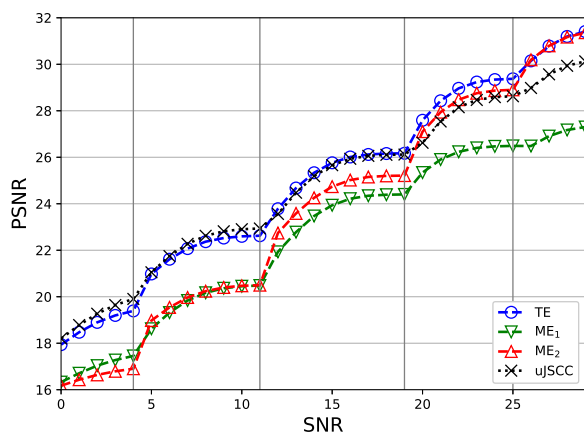
Model			Measurement		
Setting	Scheme	Modulation	FLOPs (G)	Epochs	
B	uJSCC	BPSK	0.205/0.205	178	
		4QAM	0.205/0.206		
		16QAM	0.207/0.207		
		64QAM	0.209/0.209		
	TE	256QAM	0.210/0.210	473	
		BPSK	0.205/0.205		41
		4QAM	0.205/0.206		44
		16QAM	0.207/0.207		93
64QAM	0.209/0.209	143			
256QAM	0.210/0.210	152			
L	uJSCC	BPSK	0.807/0.807	178	
		4QAM	0.811/0.811		
		16QAM	0.817/0.817		
		64QAM	0.824/0.824		
		256QAM	0.830/0.830		
	TE	BPSK	0.807/0.807	34	
		4QAM	0.811/0.811	32	
		16QAM	0.817/0.817	65	
		64QAM	0.824/0.824	125	
		256QAM	0.830/0.830	185	
MS	uJSCC	BPSK	0.324/0.324	141	
		4QAM	0.327/0.327		
		16QAM	0.334/0.334		
		64QAM	0.340/0.340		
		256QAM	0.347/0.347		
	TE	BPSK	0.324/0.324	64	
		4QAM	0.327/0.327	93	
		16QAM	0.334/0.334	100	
		64QAM	0.340/0.340	149	
		256QAM	0.347/0.347	107	

### A. Model Efficiency of uJSCC

TABLE IV shows that BN layer parameters account for only 1-2% of total model parameters, indicating that S-BN layers in uJSCC minimally impact overall model size, with ME<sub>1</sub> and ME<sub>2</sub> comprising about 98-99% of uJSCC’s parameters. Conversely, TE’s parameter count is nearly fivefold higher due to its five separate JSCC encoder-decoder pairs for each modulation order, underscoring the proposed model’s parameter efficiency.



(a) SSIM vs. SNR



(b) PSNR vs. SNR

Fig. 4. Performance comparison between uJSCC and benchmark schemes under **Basic** setting.

TABLE V details the FLOPs for the encoder and decoder during forward pass, primarily affected by the CNN layers, with nearly identical figures for uJSCC’s universal encoder and decoder. FLOPs for uJSCC are on par with TE, indicating comparable operational efficiency across all of the modulation orders. uJSCC, employing parameter sharing and joint training across modulation orders, requires far fewer training epochs than TE, which trains each modulation order separately. This efficient training approach of uJSCC leads to fewer epochs especially as TE’s training epochs increase with higher modulation orders due to greater codebook cardinality and longer codeword dimensions, highlighting uJSCC’s efficiency in training complexity.

### B. uJSCC vs. Benchmarks under **Basic** Setting

Fig. 4 demonstrates that uJSCC, with only a single universal encoder and decoder, surpasses benchmark schemes in low SNR environments when transmitting 256 symbols using BPSK and 4QAM. This highlights the advantage of semantic communication where uJSCC, benefiting from joint training and parameter sharing across multiple modulation orders, enhances image reconstruction in lower modulation

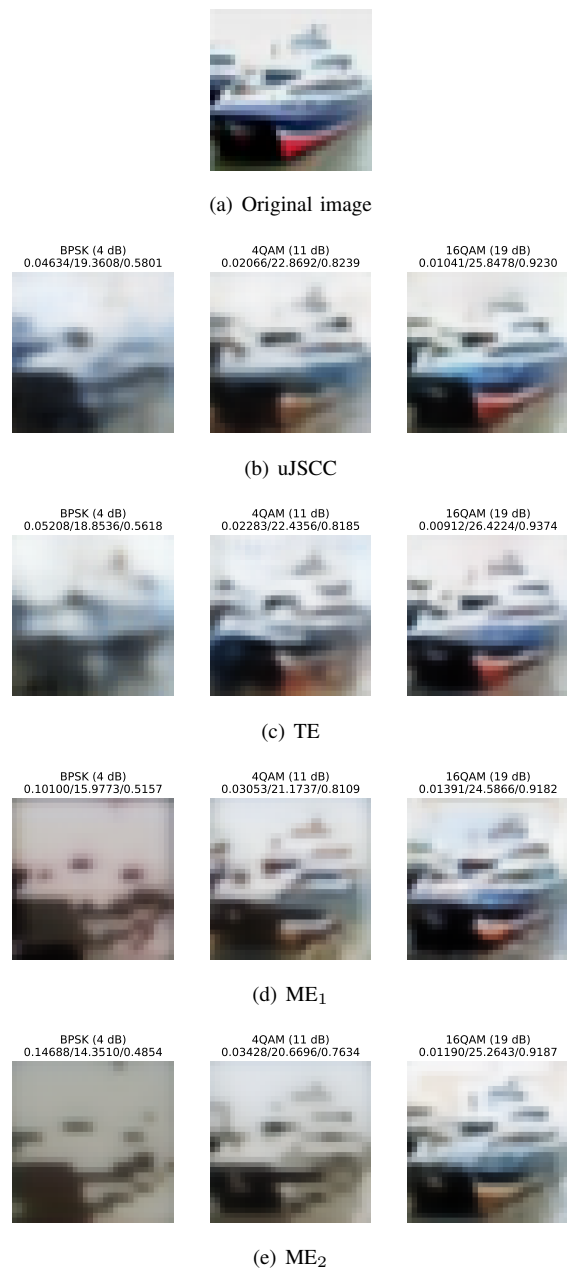
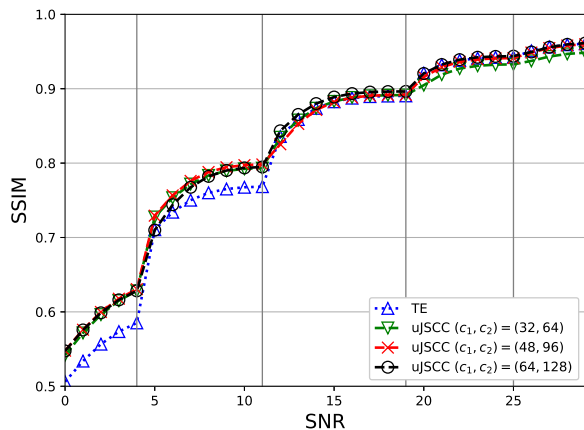


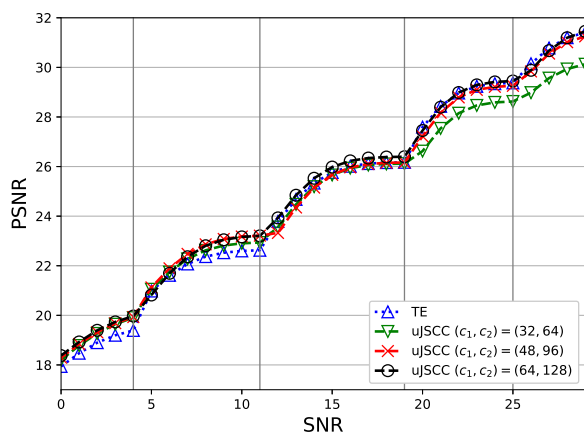
Fig. 5. Original image and reconstructed images for BPSK, 4QAM, and 16QAM (Performance is numerically written in “MSE/PSNR/SSIM” format.) under **Basic** setting.

orders using the capabilities of higher orders. ME<sub>1</sub> lacks S-BN layers, impairing its ability to equalize output tensor statistics across CNN layers for each modulation order. For higher orders like 64QAM and 256QAM, TE and ME<sub>2</sub> excel, with ME<sub>2</sub> matching TE’s performance initially trained for 256QAM, yet showing weaker performance in lower orders due to suboptimal training across remaining codebooks.

Fig. 5 displays reconstructed images from various models for BPSK, 4QAM, and 16QAM. The results for 64QAM and 256QAM are omitted as all models, except ME<sub>1</sub>, demonstrate satisfactory image quality. uJSCC clearly outperforms other models in lower modulation orders like BPSK and 4QAM. For 16QAM, uJSCC and TE show comparable and superior image



(a) SSIM vs. SNR



(b) PSNR vs. SNR

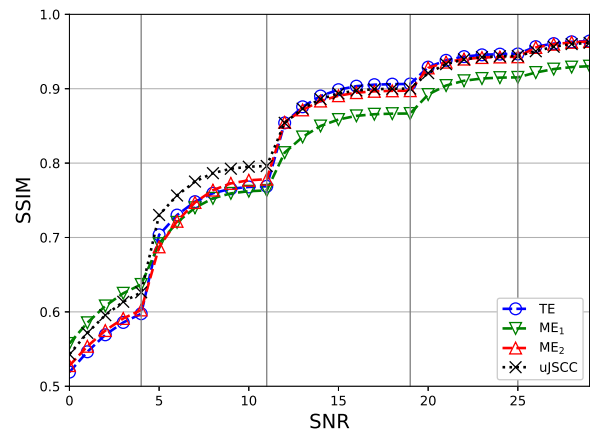
Fig. 6. Performance comparison between TE and uJSSC with different number of channels ( $N = 256$ ,  $(D_1, D_2, D_3, D_4, D_5) = (2, 4, 8, 12, 16)$ ).

quality over  $ME_1$  and  $ME_2$ , affirming uJSSC's advantage in low SNR settings through effective semantic communication.

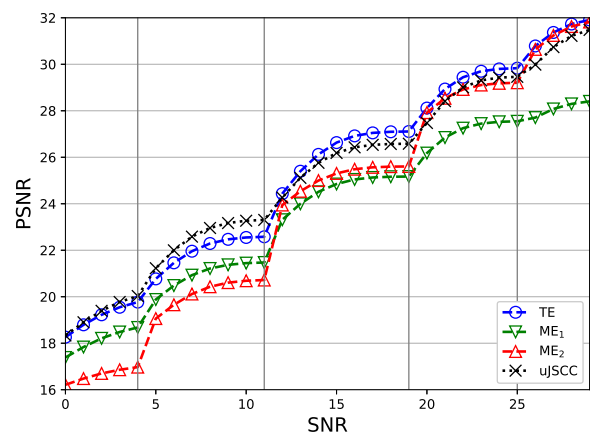
Fig. 6 assesses image reconstruction between TE and uJSSC with varying channel counts,  $c_1$  and  $c_2$ . By augmenting the number of parameters while maintaining codeword dimensions  $D_k$  for  $k \in [1:K]$ , uJSSC approaches TE's performance. Despite an increase in model size, as noted in TABLE IV, uJSSC retains fewer parameters than TE, indicating that enhancing model parameters can narrow the performance gap while remaining more parameter-efficient.

### C. uJSSC vs. Benchmarks under **Large** Setting

Fig. 7 depicts the image reconstruction performance of uJSSC and benchmark schemes using an enlarged model. This setup exhibits a trend similar to the **Basic** configuration. According to the SSIM metric, uJSSC generally outperforms except in the BPSK range, where  $ME_1$  leads narrowly but shows weaker performance across other modulation orders. Notably, uJSSC significantly surpasses other models in the 4QAM range, crucial for the visual quality of the reconstructed image.



(a) SSIM vs. SNR



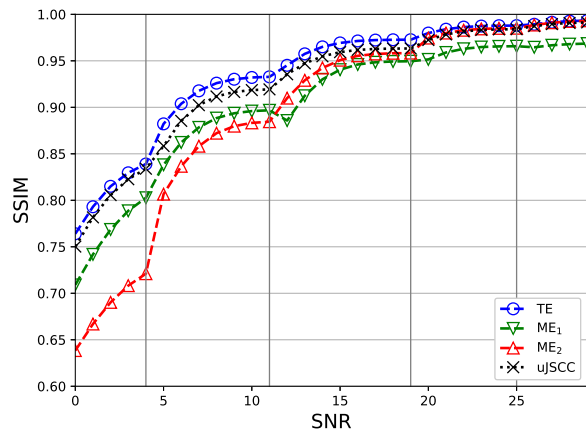
(b) PSNR vs. SNR

Fig. 7. Performance comparison between uJSSC vs. benchmark schemes under **Large** setting.

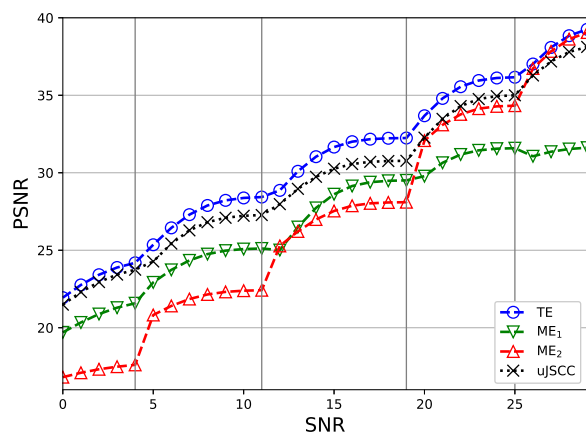
In terms of the PSNR metric, uJSSC excels in the low SNR zones like BPSK and 4QAM and closely matches TE's performance in higher modulation orders, despite TE having approximately five times more parameters. The slight PSNR shortfall in the high SNR region is not detrimental as uJSSC nearly reaches peak performance in terms of SSIM, which is more reflective of the structural integrity of the reconstructed image. Given that  $ME_1$  underperforms compared to uJSSC in the BPSK range, both SSIM and PSNR metrics are crucial for a comprehensive evaluation of the image reconstruction quality. This simulation confirms that a larger uJSSC model, when implemented with the devised training strategy, can achieve superior or competitive reconstruction across all SNR ranges with reduced training complexity relative to TE.

### D. uJSSC vs. Benchmarks under **More Symbols** Setting

Fig. 8 evaluates the image reconstruction performance of uJSSC and benchmark schemes with a transmission of 1024 symbols, i.e.,  $N = 1024$ . Transmitting more symbols enhances overall performance compared to the **Basic** setting. TE excels across all SNR ranges, as its encoder-decoder pairs are specifically trained for individual modulation orders at



(a) SSIM vs. SNR



(b) PSNR vs. SNR

Fig. 8. Performance comparison between uJSCC vs. benchmark schemes under **More Symbols** setting.

corresponding SNR levels. However, uJSCC closely rivals TE, particularly matching its performance in the high SNR region with 64QAM and 256QAM, as measured by SSIM.  $ME_1$  consistently underperforms across all SNR ranges, while  $ME_2$  performs poorly in low SNR settings with BPSK and 4QAM but well in higher SNR areas. This discrepancy highlights the challenge of optimizing a model across all SNR ranges through joint training, which is not the case for uJSCC. The effectiveness of the proposed NN structure, particularly with increased codeword dimension order and the integration of S-BN layers, alongside the training algorithm, is demonstrated in achieving high-quality outcomes for the downstream task. uJSCC maintains moderate to high performance across a broad SNR spectrum, supporting multiple modulation orders with a single universal model.

Fig. 9 presents the reconstructed images from each model for BPSK, 4QAM, and 16QAM when transmitting 1024 symbols. As higher modulation orders like 64QAM and 256QAM generally yield satisfactory results, the focus is on lower orders.  $ME_2$ , optimized only for 256QAM, shows compromised image quality in lower modulation orders despite the high symbol count.  $ME_1$  exhibits better performance in low SNR

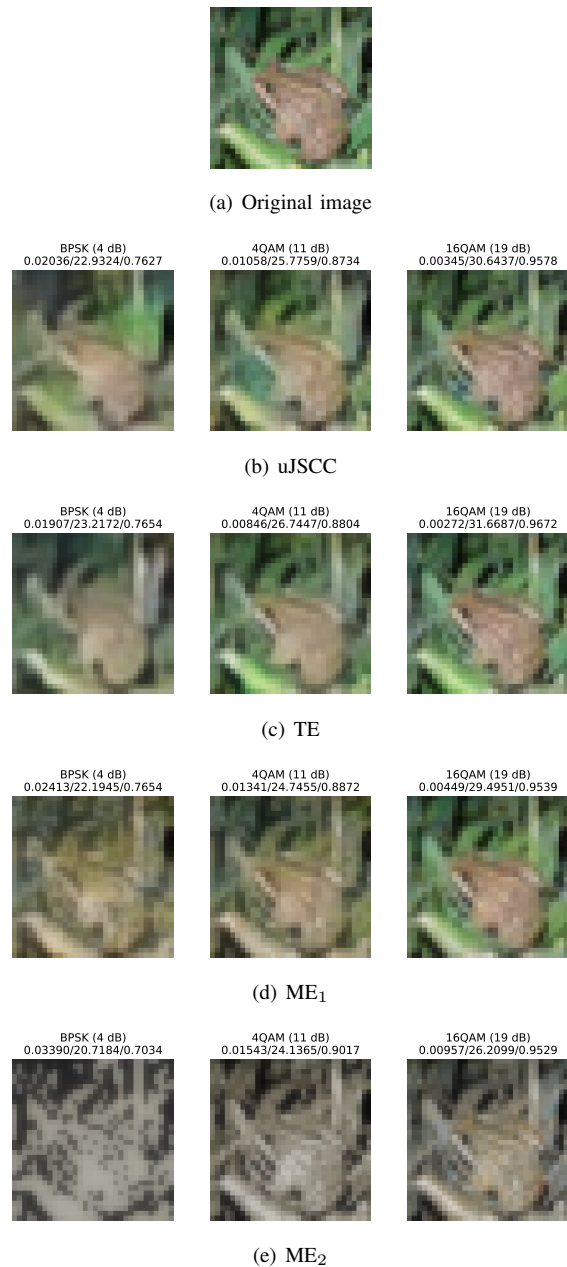


Fig. 9. Original image and reconstructed images for BPSK, 4QAM, and 16QAM (Performance is numerically written in “MSE/PSNR/SSIM” format.) under **More Symbols** setting.

regions, showcasing the strength of joint training. Nonetheless, as uJSCC mirrors TE’s optimal performance, it delivers superior image quality in low SNR regions. This simulation confirms that uJSCC, with a robustly designed NN structure and training strategy, can be optimized to maintain satisfactory task quality across all SNR ranges when transmitting a higher number of symbols.

## V. CONCLUSION

In this paper, we introduced a uJSCC framework that facilitates modulation-agnostic digital semantic communication. The data processing path within uJSCC mimics a traditional JSCC encoder-decoder pair tailored to a specific modulation

order. Utilizing parameter sharing, which enhances model efficiency, the output statistics of each CNN layer are regulated by S-BN layers tailored for each modulation order to standardize the output statistics across different data processing paths. Through our proposed joint training strategy, experimental results demonstrate that uJSCC, with significantly fewer parameters and reduced training epochs, either matches or closely approaches the task performance of traditional encodings as evaluated by metrics such as SSIM, PSNR, and the quality of reconstructed images for each modulation order. Furthermore, we have validated the versatility of uJSCC in larger models and with different numbers of transmitted symbols. Future research may explore optimizing the number of transmitted symbols or the dimensions of codewords for each modulation order. This study aims to illuminate the practical applicability of JSCC-based semantic communication using digital communication devices in real-world scenarios.

## REFERENCES

- [1] Y. Shi, Y. Zhou, D. Wen, Y. Wu, C. Jiang, and K. B. Letaief, "Task-oriented communications for 6g: Vision, principles, and technologies," *IEEE Wireless Communications*, vol. 30, no. 3, pp. 78–85, 2023.
- [2] D. Gündüz, Z. Qin, I. E. Aguerri, H. S. Dhillon, Z. Yang, A. Yener, K. K. Wong, and C.-B. Chae, "Beyond transmitting bits: Context, semantics, and task-oriented communications," *IEEE Journal on Selected Areas in Communications*, vol. 41, no. 1, pp. 5–41, 2022.
- [3] H. Seo, J. Park, M. Bennis, and M. Debbah, "Semantics-native communication via contextual reasoning," *IEEE Transactions on Cognitive Communications and Networking*, 2023.
- [4] H. Seo, Y. Kang, M. Bennis, and W. Choi, "Bayesian inverse contextual reasoning for heterogeneous semantics- native communication," *IEEE Transactions on Communications*, vol. 72, no. 2, pp. 830–844, 2024.
- [5] W. Weaver, "Recent contributions to the mathematical theory of communication," *ETC: a review of general semantics*, pp. 261–281, 1953.
- [6] X. Luo, H.-H. Chen, and Q. Guo, "Semantic communications: Overview, open issues, and future research directions," *IEEE Wireless Communications*, vol. 29, no. 1, pp. 210–219, 2022.
- [7] N. Farsad, M. Rao, and A. Goldsmith, "Deep learning for joint source-channel coding of text," in *2018 IEEE international conference on acoustics, speech and signal processing (ICASSP)*. IEEE, 2018, pp. 2326–2330.
- [8] E. Bourtsoulatzé, D. B. Kurka, and D. Gündüz, "Deep joint source-channel coding for wireless image transmission," *IEEE Transactions on Cognitive Communications and Networking*, vol. 5, no. 3, pp. 567–579, 2019.
- [9] H. Xie, Z. Qin, G. Y. Li, and B.-H. Juang, "Deep learning enabled semantic communication systems," *IEEE Transactions on Signal Processing*, vol. 69, pp. 2663–2675, 2021.
- [10] J. Xu, B. Ai, W. Chen, A. Yang, P. Sun, and M. Rodrigues, "Wireless image transmission using deep source channel coding with attention modules," *IEEE Transactions on Circuits and Systems for Video Technology*, vol. 32, no. 4, pp. 2315–2328, 2021.
- [11] Q. Hu, G. Zhang, Z. Qin, Y. Cai, G. Yu, and G. Y. Li, "Robust semantic communications with masked vq-vae enabled codebook," *IEEE Transactions on Wireless Communications*, 2023.
- [12] S. Xie, S. Ma, M. Ding, Y. Shi, M. Tang, and Y. Wu, "Robust information bottleneck for task-oriented communication with digital modulation," *IEEE Journal on Selected Areas in Communications*, 2023.
- [13] T.-Y. Tung, D. B. Kurka, M. Jankowski, and D. Gündüz, "Deepjssc-q: Constellation constrained deep joint source-channel coding," *IEEE Journal on Selected Areas in Information Theory*, 2022.
- [14] A. Van Den Oord, O. Vinyals *et al.*, "Neural discrete representation learning," *Advances in neural information processing systems*, vol. 30, 2017.
- [15] A. Dosovitskiy, L. Beyer, A. Kolesnikov, D. Weissenborn, X. Zhai, T. Unterthiner, M. Dehghani, M. Minderer, G. Heigold, S. Gelly *et al.*, "An image is worth 16x16 words: Transformers for image recognition at scale," *arXiv preprint arXiv:2010.11929*, 2020.
- [16] N. Tishby, F. C. Pereira, and W. Bialek, "The information bottleneck method," *arXiv preprint physics/0004057*, 2000.
- [17] E. Jang, S. Gu, and B. Poole, "Categorical reparameterization with gumbel-softmax," *arXiv preprint arXiv:1611.01144*, 2016.
- [18] Y. Bo, Y. Duan, S. Shao, and M. Tao, "Joint coding-modulation for digital semantic communications via variational autoencoder," *IEEE Transactions on Communications*, 2024.
- [19] H. Gao, G. Yu, and Y. Cai, "Adaptive modulation and retransmission scheme for semantic communication systems," *IEEE Transactions on Cognitive Communications and Networking*, 2023.
- [20] Y. He, G. Yu, and Y. Cai, "Rate-adaptive coding mechanism for semantic communications with multi-modal data," *IEEE Transactions on Communications*, 2023.
- [21] H. Zhang, T.-W. Weng, P.-Y. Chen, C.-J. Hsieh, and L. Daniel, "Efficient neural network robustness certification with general activation functions," *Advances in neural information processing systems*, vol. 31, 2018.
- [22] J. Park, Y. Oh, S. Kim, and Y.-S. Jeon, "Joint source-channel coding for channel-adaptive digital semantic communications," *arXiv preprint arXiv:2311.08146*, 2023.
- [23] 3GPP, "NR; Physical layer procedures for data," 3rd Generation Partnership Project (3GPP), Technical Specification (TS) 38.214, March 2024, version 18.2.0.
- [24] J. G. Proakis and M. Salehi, *Fundamentals of communication systems*. Pearson Education India, 2007.
- [25] S. Ioffe and C. Szegedy, "Batch normalization: Accelerating deep network training by reducing internal covariate shift," in *International conference on machine learning*. pmlr, 2015, pp. 448–456.
- [26] J. Yu, L. Yang, N. Xu, J. Yang, and T. Huang, "Slimmable neural networks," *arXiv preprint arXiv:1812.08928*, 2018.
- [27] D. P. Kingma and J. Ba, "Adam: A method for stochastic optimization," *arXiv preprint arXiv:1412.6980*, 2014.
- [28] A. Hore and D. Ziou, "Image quality metrics: Psnr vs. ssim," in *2010 20th international conference on pattern recognition*. IEEE, 2010, pp. 2366–2369.
- [29] K. He, X. Zhang, S. Ren, and J. Sun, "Deep residual learning for image recognition," in *Proceedings of the IEEE conference on computer vision and pattern recognition*, 2016, pp. 770–778.
- [30] A. Krizhevsky, G. Hinton *et al.*, "Learning multiple layers of features from tiny images," 2009.